

Crossover of spin glass characteristics as a function of field in an NiMnSnAl alloy

Sandeep Agarwal,¹ S. Banerjee,² and P. K. Mukhopadhyay^{1,a)}

¹*LCMP, Department of Condensed Matter Physics and Material Sciences, S.N. Bose National Centre for Basic Sciences, JD Block, Salt Lake, Kolkata 700098, India*

²*Surface Physics Division, Saha Institute of Nuclear Physics, 1/AF, Bidhan Nagar, Kolkata 700064, India*

The magnetic state in martensitic phase of Ni₅₀Mn₃₄Sn₆Al₁₀ shows interesting glassy behaviour. The irreversibility was observed in d.c. magnetization measurement below martensitic transformation temperature. Further measurements at lower temperature showed the presence of exchange bias field in sample. H-T phase diagram of the irreversibility showed that the system was in Heisenberg like spin glass state at low field, which changed its type when the external field was above the exchange bias field. In order to determine the cause of cross over, a.c. susceptibility measurements were performed in zero and d.c. biasing fields. This switching of glassy nature of the system is a novel phenomenon.

I. INTRODUCTION

Ferromagnetic shape memory alloys (FSMA) of family Ni-Mn-X (X=Ga, Sn, Sb, and In) show many promising physical properties such as large magnetic-field-induced strain, magnetoresistance, and inverse magnetocaloric effects.¹⁻⁴ The structural transformation coupled with magnetic order gives rise to these properties. However, it was found that despite having all these interesting properties, these systems are mostly too brittle for real world use. It was found that X = Al based systems have better ductility but the preparation of systems with desired property is difficult, also the transformation temperatures are quite high. This system tends to grow into B2 structure in austenitic phase, whereas for better FSMA properties, the system must be in L2₁ structure.⁵ On the other hand, Sn based system is more stable (tends to stay in L2₁ structure) so it can be easily produced in large scale. Therefore, an alloy with intermediate composition is of interest because it is expected to retain much of useful properties from both sides. We investigated one such system (nominally Ni₅₀Mn₃₄Sn₁₀Al₆) and report here the findings. Further interest in this system comes from the fact that these NiMn based Heusler alloys are known to display rich magnetic phases at low temperatures.

In the low temperature, the Ni-Mn-Sn FSMA system, within certain range of composition, shows exchange bias effect, which indicates the presence of mixed magnetic phase with ferromagnetic (FM) and antiferromagnetic (AFM) interactions.⁶⁻⁹ This mixed interaction leads to frustration that is observed as various types of glassy blocking in this system. Generally, a.c. susceptibility measurements were used to study various types of spin glass blocking in the Ni-Mn-X systems.⁸⁻¹¹ The dynamics of the glassy system can also be analyzed by studying the magnetic field temperature (H-T) phase diagram. The H-T diagram may not give a full picture about the nature of spin glass present in a system, as the usual experiments are hardly performed under

thermodynamic equilibrium as pointed out in Ref. 12; nevertheless, it reflects what kind of dynamics is involved in the freezing or defreezing process. Apart from that, there are, to our knowledge, no study on the effect of d.c. magnetic field on the spin glass freezing in FSMA alloy.

In the present work, we report on detailed study of the magnetic property of the martensitic phase of an Ni-Mn-Sn-Al alloy system. The martensite phase shows frustration and exchange bias effect. The dynamics of the system below and above this exchange bias field were explored using a.c. susceptibility technique. The H-T phase diagram of the system showed signature of Heisenberg spin glass in low field region and deviated above the exchange bias field.

II. EXPERIMENTAL DETAILS

The polycrystalline sample was prepared by melting high purity (better than 99.9%) constituent elements in an arc furnace under flowing argon atmosphere. The sample was turned and melted several times to insure homogeneity. It was then sealed in an evacuated quartz tube and annealed at 1273 K for 72 h, followed by quenching in ice water. The X-ray diffraction (XRD) (Rigaku MiniFlexIITM) was performed on powdered sample using Cu K_α ($\lambda = 0.154$ nm) radiation. The Differential Scanning Calorimeter (DSC) measurement was performed during heating and cooling at the rate of 10 K min⁻¹ using a Thermal Analysis Q-2000TM instrument. Magnetization measurements were performed using a Quantum Design SQUID magnetometer (MPMS EverCoolTM model). AC susceptibility measurements were performed in r.m.s. fields of 40 Oe in a home made setup of mutual inductance bridge and in 3 Oe using the SQUID.

III. RESULTS AND DISCUSSION

In Figure 1(a), XRD pattern at 300 K is shown. The Rietveld refinement shows the presence of single cubic phase at room temperature having L2₁ structure with calculated lattice parameter as 0.593 nm, which is less than similar compositions Ni₅₀Mn₃₄Sn₁₆ (0.599 nm) and the Ni₅₀Mn₃₄Sn₁₀Ga₆

^{a)}Electronic mail: pkm@bose.res.in

alloys (0.594 nm).¹³ Since the fit is reasonably good in L2₁ structure and only even order reflections are present at high angles, these imply that the disorder, which was brought about by the chemical substitutions of Sn by Al, was only marginal and did not bring into the system a significant amount of B2 phase. The fact that the L2₁ structure was preserved in this system even after quenching from high temperature is in confirmation to the idea that substitution of bigger atoms in place of Al and Mn would stabilize this structure against B2.¹⁴ Further information than this will need a neutron diffraction experiment. The DSC plot, shown in Figure 1(b), confirms the structural transitions. The characteristic transition temperatures, viz., martensite start (T_{Ms}), martensite finish (T_{Mf}), austenite start (T_{As}), and austenite finish (T_{Af}), were determined from exothermic (cooling) and endothermic (heating) peaks to be 171 K, 158 K, 168 K, and 196 K, respectively. (These temperatures were determined from the intersections of straight lines extrapolated from both sides of the bends in the curves. Indeed, this is the method used for determination of all temperatures from the graphs.) There was a small kink at 326 K corresponding to Curie temperature, T_c. The T_{Mf} of the present sample lies between those of Ni₅₀Mn₃₄Sn₁₆ (Ref. 13) (110 K) and Ni₅₀Mn₃₄Al₁₆ (Ref. 15) (~415 K). This is consistent with the argument that replacement of Sn with an element having smaller radius would increase the transition temperature due to lattice compression, even though valance electron concentration decreased.¹³

The Zero-field-cooled (ZFC), field-cooled (FC), and field-heated (FH) thermo-magnetizations were performed

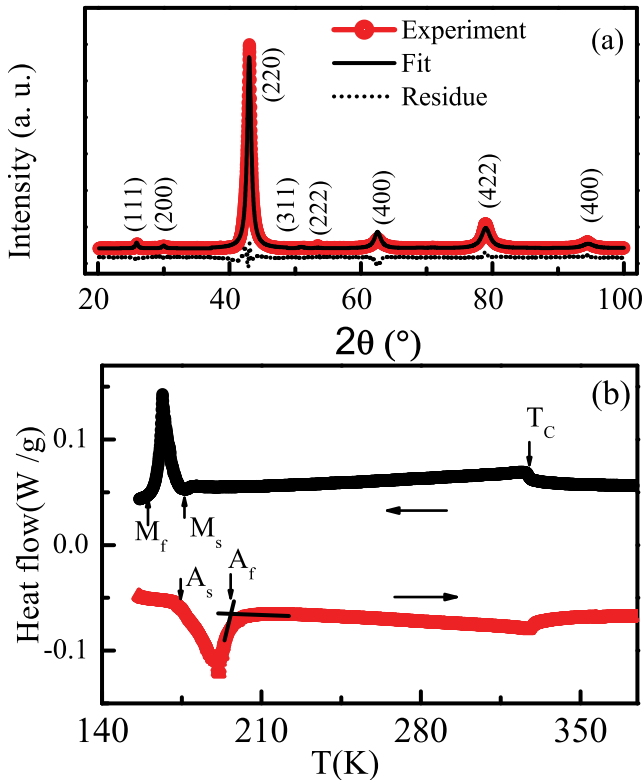


FIG. 1. (a) Room temperature XRD pattern along with the fitted pattern and residue. (b) DSC curve as function of temperature. One of the straight line intersections are shown, which was used to determine the transition temperatures.

in external field of 500 Oe and are shown in Figure 2(a). Following general trends for the L2₁ structure of Ni₂MnX family, it was found to be ferromagnetic, with T_c = 331 K, as determined from 1/χ' ~ T plot (shown in inset in the in Figure 2(a)), obtained from a.c. susceptibility measurement done at 111 Hz. The temperatures for fall and rise of M during cooling and heating coincided within ±5 K of the structural transformation temperatures determined from DSC. It is known that in the stoichiometric Ni₂MnX alloy the Mn-Mn interaction is ferromagnetic, whereas in off-stoichiometric Ni-Mn-X alloy, the excess Mn in X site interacts with Mn in regular site antiferromagnetically. The AFM interaction comes into play with martensitic transformation and enhanced as temperature is lowered.¹⁶ This results in coexistence of both AFM and FM interactions in martensite phase (MP), which explains the appearance of irreversibility in ZFC and FC thermo-magnetization curve.^{7,8} In order to ascertain the magnetic nature of MP at low temperature, isothermal magnetic hysteresis (M-H) measurements were performed at 5 K after ZFC as shown in Figure 2(b) (inset shows only from -0.1 T to 0.1 T for clarity). The ZFC M-H curve shows symmetric double shifted loop which has been observed in off stoichiometric Ni-Mn-Sn samples.⁹ The double shifted loop vanished when M-H measurement was performed after ZFC at 30 K. Double shifted loops are observed in a system that has AFM-FM interface—when the sample is zero field cooled, the AFM region gets divided into two types of regions

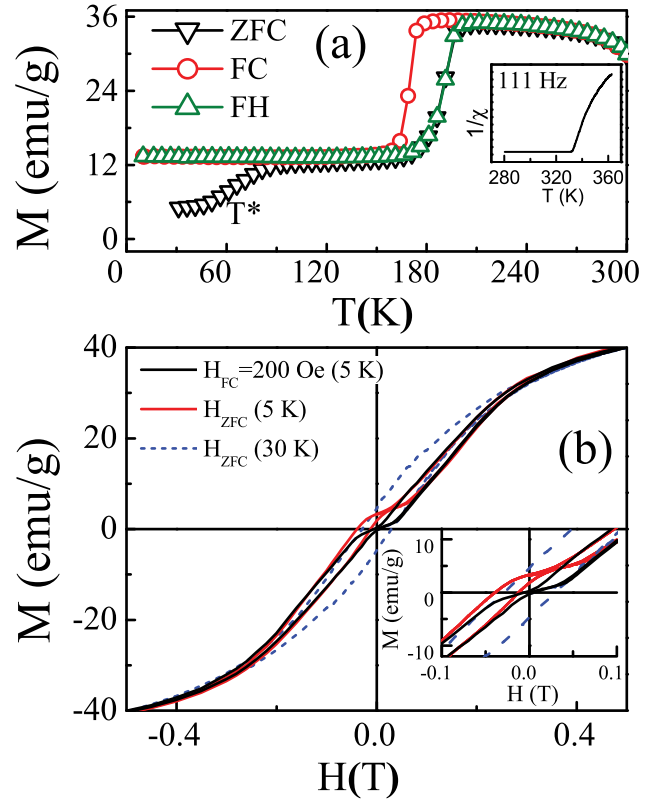


FIG. 2. (a) ZFC, FC, and FH at the field of 500 Oe as a function of temperature. The inset in 2 (a) shows inverse real χ' at 111 Hz. (b) Full MH curve measured after FC at 200 Oe and ZFC at different temperatures. The inset in Fig. 2(b) shows the expanded region near zero field.

which are locally oriented in opposite direction. The AFM regions pin various FM regions in opposite ways, resulting in shift of one sub-loop towards the positive-field axis while other sub-loop shifts towards the negative direction, giving rise to double shifted loops.^{7,9} This interaction also leads to shift in hysteresis loop along the field axis when sample is field cooled and is known as Exchange Bias (EB) effect. In order to confirm EB-effect, M-H was performed at 5 K after FC at 200 Oe, in fields ranging from +1 T to -1 T, which are much above the saturation field. The sample shows EB-effect in which M-H curve is asymmetric and loop shifts both horizontally and vertically. The horizontal shift (H_E), which gives EB-field, is about 250 Oe. Here, $H_E = -(H_1 + H_2)/2$, where H_1 and H_2 are the left and right coercive fields, respectively. The vertical shift in the M-H curve also implies that double shifted loop and EB arise due to the presence of glassy magnetic phase.⁶

To further investigate this region, ZFC measurements were performed under fields varying from 10 Oe to 2 kOe. The value of T^* , defined as the temperature when magnetization started to rise in ZFC as temperature increased, was measured by line intersection method as before. The value of T^* for each field was obtained, and the resultant H-T phase diagram is shown in Figure 3. As the field was increased, T^* fell rapidly until 300 Oe, above which change in T^* was very small. This seems to imply that the applied field matched the locking internal field, above which the unlocked domains could move in response to the applied field. Beyond this, the M will now vary as a function of the difference between H and the anisotropic field. This unlocking was also indicated by the disappearance of the double shifted loop in hysteresis at 30 K.

This unpinning of the FM domains, along with the presence of AFM also means that just above T^* the system would behave like a spin glass in the canonical sense. The irreversible nature has also been studied using d.c. magnetization technique. The field dependent shift of T^* is generally described as $H(T) \propto [1 - T^*(H)/T(0)]^\gamma$, where $T(0)$ is limiting temperature at zero field. Here, the parameter γ is to indicate if the system is isotropic Ising like spin glass ($\gamma = 3/2$) or Heisenberg like ($\gamma = 1/2$).¹⁷ The variation of $\gamma = 3/2$ and $\gamma = 1/2$ reflect different dynamics occurring in the spin glass system during freezing process. The transverse components of the spin freeze along the $\gamma = 1/2$ and the longitudinal spin

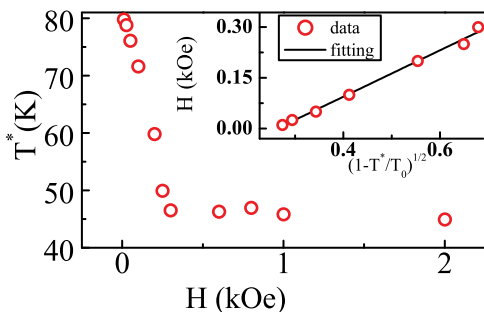


FIG. 3. H-T phase diagram, T^* is the freezing temperature at a given field. The inset shows fitting to Heisenberg model, up to 300 Oe as a function of reduced temperature.

component freeze along the $\gamma = 3/2$ line.¹² We plotted in Figure 3 the variation of H-T at this temperature range. It can be seen that the initial fast variation of T^* at low field was stuck above about 300 Oe. In the inset, we show the fit at lower field with the above equation, the fit was excellent with $\gamma = 1/2$, implying that as the temperature increased the transverse component of the spin glass relaxes first. Recent study on the Ni-Mn-Co-In system showed that system froze along $\gamma = 3/2$ line but in that case, the spin glass came from Para-Spin glass transition,¹⁸ whereas in our case the spin glass if present must be of reentrant spin glass nature given that martensitic phase showed ferromagnetic characteristic much above the T^* . In addition, the sharp change was an indication that above the 300 Oe field, the barrier of the bias field was overcome and it was no longer under thermal control, in line with our earlier discussion. To understand the cause of breakdown of $\gamma = 1/2$ line in H-T phase diagram and the exact nature of glassy phase, a.c. susceptibility measurement was performed next.

To study the relaxations in the spin glass phase, frequency dependent susceptibility measurements were performed in the range from 11 Hz to 1 kHz. The real (χ') and imaginary (χ'') parts of susceptibility are shown in Figures 4(a) and 4(b), respectively. As the frequency of measurement increased, peaks in the χ'' curves were shifted to higher temperatures. The T_f was determined at the maximum of χ'' . The shift of T_f (ΔT_f) per decade of frequency change is parameterized as $\Phi = \Delta T_f / (T_f \Delta \log f)$, where f is the measuring frequency¹⁹ and provide a criterion to distinguish spin glass freezing and superparamagnetic blocking. It was experimentally found to be a small number, but nevertheless some distinct ranges could be found. While the range is below 0.01 for other magnetically dilute alloys, for alloys of Mn with

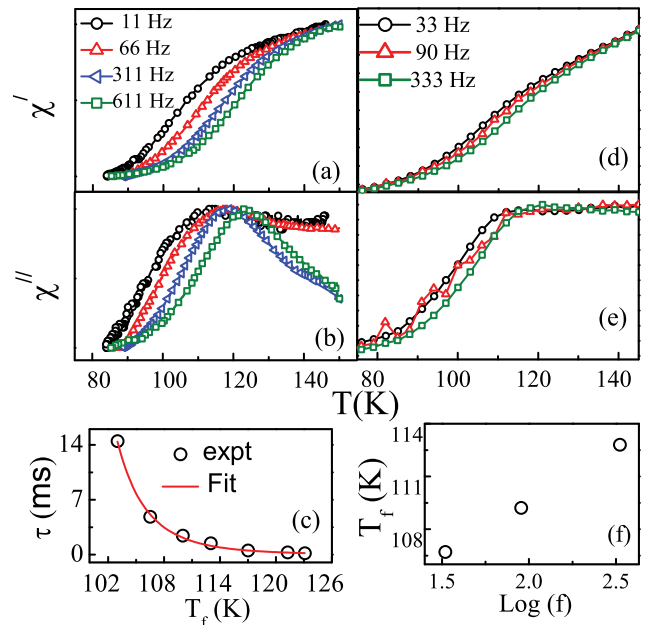


FIG. 4. Normalized frequency dependent (a) real (χ') and (b) imaginary (χ'') of a.c. susceptibility as a function of temperature in zero d.c. field. Figure (c) shows experimental data fitted with dynamical scaling law for phase transition. Figs. (d) and (e) show χ' and χ'' at 700 Oe d.c. field and Figure (f) shows shift of T_f with frequency at d.c. field of 700 Oe.

another transition metal, it comes to higher values, like 0.025,²⁰ and for concentrated alloys and insulating glasses, it can range up to 0.08. On the other hand, it can go up to 0.3 for superparamagnets. In our case, the fitting gives the value of Φ as 0.094. This value is on the rather higher side, and raises the suspicion on the system being on the borderline of superparamagnet (SPM). This is even more possible, for it is known that the high values can come from ferromagnetic clustering.²⁰ However, there are other checks for it. We tried to fit the M-H loop at 30 K with Langevin function,¹¹ but the fit gave a unphysical negative value of susceptibility so that we had to conclude that the SPM was unlikely. Next, the data were fitted to the Arrhenius law,⁸ $\omega = \omega_0 \exp(-E_a/k_B T_f)$, where $\omega = 2\pi f$, E_a being the activation energy and ω_0 being the characteristic frequency. The fitted parameters E_a and ω_0 were found to be 3000 K and $3 \times 10^{13} \text{ s}^{-1}$, respectively. These unphysical values imply that the system was in the spin glass kind of state. To obtain characteristic time scale of activation near T_f , we analyzed the result using $\tau = \tau^* (T_f/T_0 - 1)^{-z\nu}$, as a standard theory of dynamical scaling near the phase transition.²¹ The result is shown in Figure 4(c), where $\tau = 1/f$, T_0 is freezing temperature as frequency and field tend to zero, while $z\nu$ is dynamical exponent and τ^* is macroscopic relaxation time related to spin glass or cluster glass phase. The values obtained for τ^* and $z\nu$ were $1.2 \times 10^{-5} \text{ s}$ and 5.5, respectively. The value of $z\nu$ lies within 4–12 for spin glass system, whereas τ^* is of the order of 10^{-12} – 10^{-14} s .¹² Such a large value of τ^* coupled with the larger value of Φ would imply a slow dynamics in the system, due to the presence of a small internal retarding field, similar to the reported previously in the context of an assembly of interacting particle system.²¹ This indicates that system is in cluster spin glass state at this low temperature region.

To further study the nature of irreversibility and the cause of the breakdown (at field $> 300 \text{ Oe}$) in the H-T phase diagram, we performed a.c. susceptibility measurements with a d.c. bias field of 700 Oe (FC) in the SQUID magnetometer, and the results are shown in Figures 4(d) and 4(e). In this case, the extent of responses of both χ'' and χ''' becomes less spread out than before. Additionally, we note a striking feature that the peaks of χ''' were now lost in the higher temperature side. It is now not possible to find T_f from the peak, so we need to find it from the first fall of χ''' . A plot of this temperature as a function of $\log(f)$, shown in Figure 4(f), finds a linear dependence and fit to the Arrhenius law gives E_a and ω_0 as 4430 K and $2.37 \times 10^{20} \text{ s}^{-1}$, respectively, again unphysical values. The simple spin glass models therefore no longer described the system above the region of breakdown region. We conjecture that under external field, the system turned over from one kind of irreversibility to another kind. This is a completely new finding for the FSMA materials as far as our knowledge go.

IV. CONCLUSION

We made a new FSMA system with some desirable physical properties. We found that it had transition temperatures

significantly higher than Sn-only based systems and was more stable in austenite phase than Al-only system. Additionally, we investigated its interesting magnetic properties by various magnetization and susceptibility measurements. We found that while near room temperature it has para to ferromagnetic transition, it shows ferro-spin glass properties after structural transitions take place. It was also shown that the system shows Heisenberg like spin glass nature that changes nature above the exchange bias field. This is a novel switching behavior that was not reported before.

ACKNOWLEDGMENTS

One of the authors, S.A., thanks CSIR for financial support. Authors are thankful to UGC-DAE Consortium for Scientific Research, Kolkata Centre for helping us in some of the magnetic measurements with their SQUID facility.

- ¹R. Kainuma, Y. Imano, W. Ito, Y. Sutou, H. Morito, S. Okamoto, O. Kitakami, K. Oikawa, A. Fujita, T. Kanomata, and K. Ishida, *Nature* **439**, 957 (2006).
- ²K. Koyama, H. Okada, K. Watanabe, T. Kanomata, R. Kainuma, W. Ito, K. Oikawa, and K. Ishida, *Appl. Phys. Lett.* **89**, 182510 (2006).
- ³K. Koyama, K. Watanabe, T. Kanomata, R. Kainuma, K. Oikawa, and K. Ishida, *Appl. Phys. Lett.* **88**, 132505 (2006).
- ⁴T. Krenke, E. Duman, M. Acet, E. F. Wassermann, X. Moya, L. Mañosa, and A. Planes, *Nature Mater.* **4**, 450 (2005).
- ⁵L. Mañosa, A. Planes, M. Acet, E. Duman, and E. F. Wassermann, *J. Appl. Phys.* **93**, 8498 (2003).
- ⁶H. C. Xuan, Q. Q. Cao, C. L. Zhang, S. C. Ma, S. Y. Chen, D. H. Wang, and Y. W. Du, *Appl. Phys. Lett.* **96**, 202502 (2010).
- ⁷M. Khan, I. Dubenko, S. Stadler, and N. Ali, *Appl. Phys. Lett.* **91**, 072510 (2007).
- ⁸S. Chatterjee, S. Giri, S. De, and S. Majumdar, *Phys. Rev. B* **79**, 092410 (2009).
- ⁹S. Chatterjee, S. Giri, S. K. De, and S. Majumdar, *J. Phys.: Conf. Ser.* **200**, 032011 (2010).
- ¹⁰R. Y. Umetsu, A. Fujita, W. Ito, T. Kanomata, and R. Kainuma, *J. Phys.: Condens. Matter* **23**, 326001 (2011).
- ¹¹D. Y. Cong, S. Roth, J. Liu, Q. Luo, M. Pötschke, C. Hürrieh, and L. Schultz, *Appl. Phys. Lett.* **96**, 112504 (2010).
- ¹²A. Mauger, J. Ferré, M. Ayadi, and P. Nordblad, *Phys. Rev. B* **37**, 9022 (1988).
- ¹³S. Chatterjee, S. Giri, S. De, and S. Majumdar, *J. Alloys Compd.* **503**, 273 (2010).
- ¹⁴B. R. Coles, W. Hume-Rothery, and H. P. Myers, *Proc. R. Soc. London, Ser. A* **196**, 125 (1949).
- ¹⁵T. Inoue, S. Morito, Y. Murakami, K. Oda, and K. Otsuka, *Mater. Lett.* **19**, 33 (1994).
- ¹⁶P. J. Brown, A. P. Gandy, K. Ishida, R. Kainuma, T. Kanomata, K.-U. Neumann, K. Oikawa, B. Ouladdiaf, and K. R. A. Ziebeck, *J. Phys.: Condens. Matter* **18**, 2249 (2006).
- ¹⁷X. S. Ling and J. I. Budnick, in *Magnetic Susceptibility of Superconductors and Other Spin Systems*, edited by R. A. Hein, T. L. Francavilla, and D. H. Liebenberg (Plenum Press, New York, 1991), p. 377.
- ¹⁸J. I. Pérez-Landazábal, V. Recarte, V. Sánchez-Alarcos, C. Gómez-Polo, and E. Cesari, *Appl. Phys. Lett.* **102**, 101908 (2013).
- ¹⁹J. A. Mydosh, *Spin Glasses: An Experimental Introduction* (Taylor & Francis, London, Washington, DC, 1993).
- ²⁰G. V. Lecomte, H. von Lohneysen, and E. F. Wassermann, *Z. Phys. B* **50**, 239 (1983).
- ²¹C. Djurberg, P. Svedlindh, P. Nordblad, M. Hansen, F. Bødker, and S. Mørup, *Phys. Rev. Lett.* **79**, 5154 (1997).